J Therm Anal Calorim (2013) 112:1191–1198
DOI 10.1007/s10973-012-2640-8

Thermal decomposition of polycrystalline $[Ni(NH_3)_6](NO_3)_2$

Edward Mikuli · Anna Migdał-Mikuli · Dorota Majda

Received: 14 May 2012 / Accepted: 13 August 2012 / Published online: 28 September 2012

Abstract The thermal decompositions of polycrystalline samples of $[Ni(NH_3)_6](NO_3)_2$ were studied by thermogravimetric analysis with simultaneous gaseous products of the decomposition identified by a quadruple mass spectrometer. Two measurements were made for samples placed in alumina crucibles, heated from 303 K up to 773 K in the flow (80 cm^3 min^{-1}) of Ar 6.0 and He 5.0, at a constant heating rate of 10 K min^{-1}. Thermal decomposition process undergoes two main stages. First, the deamination of $[Ni(NH_3)_6](NO_3)_2$ to $[Ni(NH_3)_2](NO_3)_2$ occurs in four steps, and $4NH_3$ molecules per formula unit are liberated. Then, decomposition of survivor $[Ni(NH_3)_2](NO_3)_2$ undergoes directly to the final decomposition products: NiO_{1+x}, N_2, O_2, nitrogen oxides and H_2O, without the formation of a stable $Ni(NO_3)_2$, because of the autocatalytic effect of the formed NiO_{1+x}. Obtained results were compared both with those published by us earlier, by Farhadi and Roostaei-Zaniyani later and also with the results published by Rejitha et al. quite recently. In contradiction to these last ones, in the first and second cases agreement between the results was obtained.

Keywords Hexammine Werner-type complex $[Ni(NH_3)_6](NO_3)_2$ · Thermal decomposition · Thermogravimetry · Quadruple mass spectrometry · Infrared and Raman spectroscopy

Introduction

The Werner-type hexammine coordination compounds are very interesting materials to study for several reasons. One of these is their rich phase polymorphism and its connection with the structural and dynamical properties of these compounds (for example see [1, 2]). Another reason is connected with their application in medicine as compounds interacting with DNA, and as anticancer drugs [3–5]. The next important reason is that the rich family of $[M(NH_3)_n]A_m$ complexes represent the large number of compounds that can potentially be used for reversible, indirect hydrogen storage. Furthermore, they are found to exhibit facile ammonia release kinetics [6]. In addition, recently, these compounds have also been proposed as an ideal ammonia storage in connection with selective catalytic reduction (SCR) of NO_x systems [7] in both diesel and lean-burn gasoline-driven automobiles.

The synthesis, chemical composition, crystal structure, phase polymorphism, vibrational spectra and other physical and physicochemical properties of $[Ni(NH_3)_6](NO_3)_2$ have been widely described in many papers (for example see [8–19]). The thermal decomposition of $[Ni(NH_3)_6](NO_3)_2$ in a flow of Ar was first studied in 2004 by Migdał-Mikuli et al. [20]. Next, this compound was thermally decomposed in air atmosphere by Farhadi and Roostaei-Zaniyani [21] in 2011 and quite recently (2012) it was thermally decomposed in a flow of He by Rejitha et al. [22]. Because of some discrepancies in the results obtained by us and by these last authors, we have decided to repeat thermal decomposition measurements of this compound, in the presence of both Ar and He, with the same experimental conditions in both cases.

Experimental procedure

The identification of the hexamminenickel(II) nitrate(V), measured by us with formula $[Ni(NH_3)_6](NO_3)_2$, is

E. Mikuli (✉) · A. Migdał-Mikuli · D. Majda
Faculty of Chemistry, Jagiellonian University, Ingardena 3, 30-060 Kraków, Poland
e-mail: mikuli@chemia.uj.edu.pl

guaranteed by the results described in many papers mainly for three reasons. The first reason is that the present compound measured by us is exactly the same compound as the one that was measured in our papers [8–12]. The second reason is based on chemical, spectral and structural analysis of this compound. The results all of these analyses confirm its proper composition and structure. The third reason is that properties of the investigated compound are exactly identical to those which were discovered by other authors [13–19]. Unfortunately, contrary to us [20], Rejitha et al. [22] did not prove the proper composition of the compound measured by them. This could be one of the reasons why our results are somewhat different to theirs.

A characterization of the decomposition process of the $[Ni(NH_3)_6](NO_3)_2$ compound was performed using a Mettler Toledo TGA/SDTA 851^e apparatus. Evolved gaseous products from the decomposition of the compound were identified using a ThermoStar GSD300T Balzers quadruple mass spectrometer (QMS). The TGA instrument was calibrated with indium, zinc and aluminium. Its accuracy is equal to 10^{-6} g. The mass spectrometer was operated in electron impact mode (EI) using channeltron as a detector. Screening analyses were performed in the selected-ion monitoring (SIM) mode. The following ions' characteristics of each molecules, such as 17, 18, 28, 30, 32, 44 and 46, for NH_3, H_2O, N_2, NO, O_2 N_2O and NO_2, respectively, were monitored. It is important to notice that the QMS spectrum of mass 17 can represent not only NH_3 but also the OH^- fragment of H_2O fragmentation.

For the thermogravimetric analysis (TG/DTG), the samples were placed in alumina crucible. Two measurements were made: one in a flow (80 cm^3 min^{-1}) of Ar 6.0 and the second in He 5.0 in the temperature range from 30 °C up to 500 °C (303–773 K), at a constant heating rate of 10 K min^{-1}. Simultaneously, differential thermal analysis (SDTA) measurements were carried out.

Fourier-transform far and middle infrared absorption measurements (FT-FIR, FT-MIR) were performed using a Bruker VERTEX 70v vacuum spectrometer. The spectra were collected with a resolution of 2 cm^{-1} and with 64 scans per each spectrum. The FT-FIR spectra (525–100 cm^{-1}) were collected for a sample suspended in Apiezon N grease and placed on a polyethylene (PE) disc. The FT-MIR spectra (4,000–500 cm^{-1}) were recorded for the sample in KBr pellet.

The Raman spectra (RS) were recorded using a WITec confocal CRM alpha 300 Raman microscope equipped with an air-cooled solid-state laser operating at 488 nm and a CCD detector. 500 scans were registered. The power of the laser at the sample position was 40 mW and explored time was 0.5 s.

Result and discussion

In Fig. 1, TG and DTG curves of the thermal decomposition process of the studied sample obtained in Ar and in He atmosphere were plotted. They exhibited a very similar character, which indicates that the decomposition process is not influenced by a gas used in the experiment. The main difference can be observed in the temperature of the DTG peaks. Namely, the decomposition in He generally occurs in temperatures of about 20 °C lower in comparison with the experiment carried out in Ar atmosphere. It is understandable because the thermal conductivity of He is almost nine times greater than that of Ar. Figure 2 presents mass loss valued on TG curve of the $[Ni(NH_3)_6](NO_3)_2$ sample measured in He atmosphere. Figures 3, 4 and 5 present TG curve and QMS curves of the particular gaseous products of $[Ni(NH_3)_6](NO_3)_2$ thermal decomposition in He. The TG and DTG curves presented in Fig. 2 show that the decomposition of the sample proceeds in three main stages: I, II and III (each of them is composed from two steps—a and b). Table 1 presents temperature ranges, percentage mass losses and identified products of the thermal decomposition of $[Ni(NH_3)_6](NO_3)_2$. From the QMS spectra (see Figs. 3, 4), it can be observed that the stages I and II involve mainly the step-wise (Ia, Ib and IIa, IIb) freeing of $4NH_3$ molecules, whereas the stage III illustrates the decomposition of $[Ni(NH_3)_2](NO_3)_2$ to the H_2O, N_2, NO, N_2O (see Figs. 3, 4), oxygen and NO_2 (see Fig. 5) and solid NiO. The mass losses for particular step of thermal decomposition was determined from TG and DTG curves in a manner presented in Fig. 2.

Figure 6 presents the profiles of TG, DTG and SDTA curves of $[Ni(NH_3)_6](NO_3)_2$. In the temperature range of 60 to 240 °C, the SDTA curve shows four small, broad

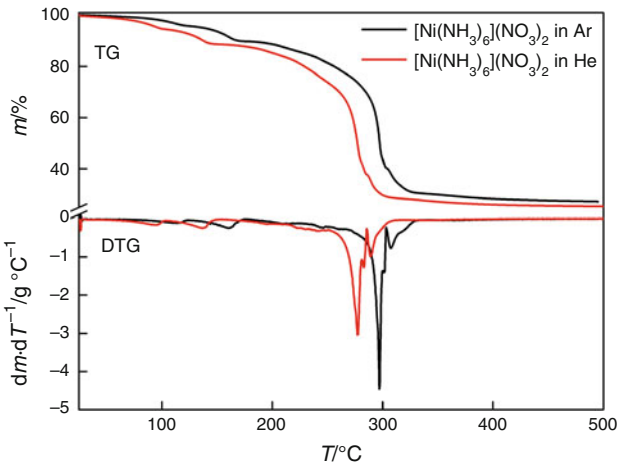

Fig. 1 TG and DTG curves of the $[Ni(NH_3)_6](NO_3)_2$ sample measured in Ar and in He atmosphere

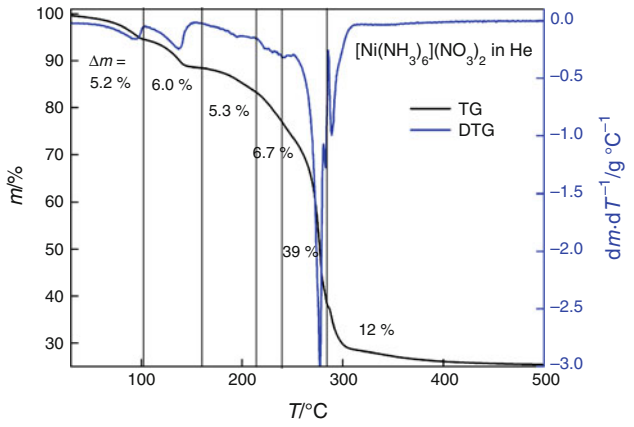

Fig. 2 Mass loss valued on TG curve of the $[Ni(NH_3)_6](NO_3)_2$ sample measured in He atmosphere

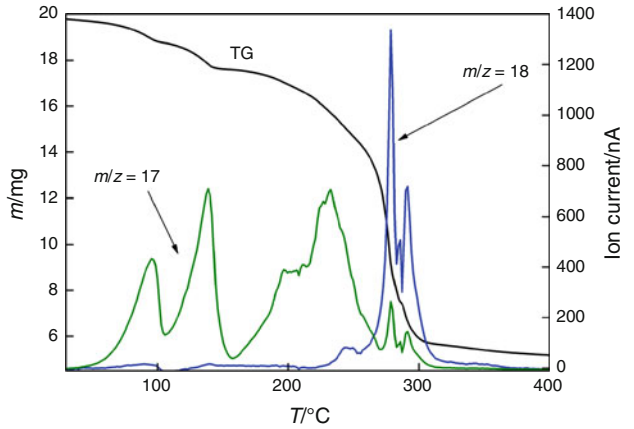

Fig. 3 TG and QMS curves of thermal decomposition of $[Ni(NH_3)_6](NO_3)_2$ in a flow of He obtained for NH_3 and H_2O species

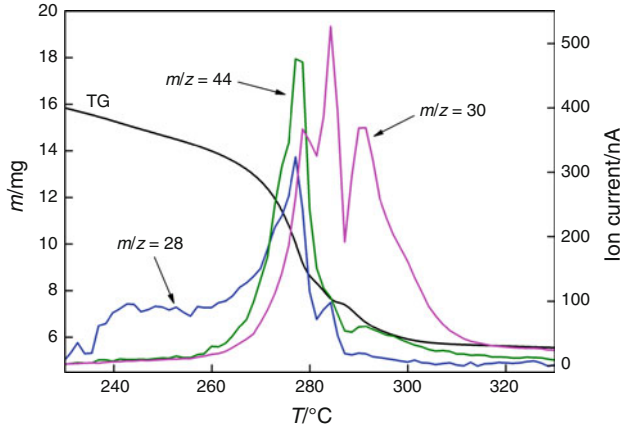

Fig. 4 TG and QMS curves of thermal decomposition of $[Ni(NH_3)_6](NO_3)_2$ in a flow of He obtained for N_2, NO and N_2O species

endothermic peaks illustrating the deamination process, one big, sharp and broad exothermic peak in the temperature range of 240–285 °C and another big, sharp and

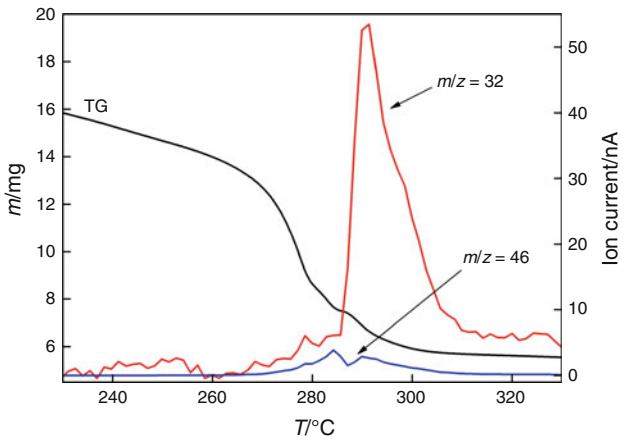

Fig. 5 TG and QMS curves of thermal decomposition of $[Ni(NH_3)_6](NO_3)_2$ in a flow of He obtained for O_2 and NO_2 species

broad but endothermic peak in the temperature range of 285–315 °C.

The exothermic peak can be explained by reduction and oxidation (redox) processes taking place between the reductant (NH_3) and the oxidant (NO_3^-). The beginning of the exothermic effect (at ca. 240 °C) is correlated with beginning of N_2 evolution observed as QMS curve $m/z = 28$ presented in Fig. 4. As can be seen in Fig. 6, the acceleration of exothermic effect is bounded with acceleration of N_2 production and with additional evolution of N_2O (curve $m/z = 44$) and with the beginning of NO ($m/z = 30$) and H_2O ($m/z = 18$) evolution. All of them starting above a temperature of 260 °C. Next, above 285 °C, the endothermic peak on DTA curve is correlated with the evolution of O_2 ($m/z = 32$) and NO_2 ($m/z = 46$), which is presented in Fig. 5, besides former evolution of H_2O and NO (see Figs. 3, 4).

Taking advantage of the results of our previous investigations [20, 23–26] and taking into account the results obtained by other researchers [27–36], the redox process, which takes place during thermal decomposition of $[Ni(NH_3)_6](NO_3)_2$, determines that this decomposition may be presented as the following reactions:

$$\text{I } \left[Ni(NH_3)_6\right](NO_3)_2 \rightarrow \left[Ni(NH_3)_4\right](NO_3)_2 + 2NH_3, \quad (1)$$

$$\text{II } \left[Ni(NH_3)_4\right](NO_3)_2 \rightarrow \left[Ni(NH_3)_2\right](NO_3)_2 + 2NH_3, \quad (2)$$

$$\text{III } \left[Ni(NH_3)_2\right](NO_3)_2 \rightarrow NiO + \frac{1}{2}O_2 + N_2 + N_2O + 3H_2O \leftrightarrow NiO + \frac{1}{2}N_2 + N_2O + NO + 3H_2O. \quad (3)$$

In order to prove that $[Ni(NH_3)_2](NO_3)_2$ is really an intermediate product of a thermal decomposition of

Table 1 Comparison of temperature ranges, percentage mass losses and identified products of the thermal decomposition of $[Ni(NH_3)_6](NO_3)_2$ obtained in four different investigations

Stage numbers	Temperature ranges (°C)					Mass loss (%)						Products of thermal decomposition					
	This study		[20]	[21]	[22]	This study		[20]	[21]	[22]	Calculated	This study		[20]	[21]	[22]	
	Ar	He	Ar	Air	He	Ar	He	Ar	Air	He		Ar	He	Ar	Air	He	
Ia	25–125	25–105	27–202	0–167	78–116	4.4	5.2	12.0	[a]	[a]	5.98	NH_3		$2NH_3$	$2NH_3$	NH_3	
Ib	126–180	106–160			116–164	6.0	6.0			[a]	5.98	NH_3				NH_3	
IIa	181–234	161–214	203–234	168–207	164–300	5.2	5.3	6.3	[a]	[a]	5.98	NH_3		NH_3	$2NH_3$	$4NH_3 + NO_3^{\bullet} + NO_2$	
IIb	235–264	215–239	235–272			7.0	6.7	6.0			5.98	NH_3		NH_3			
IIIa	265–285	240–285	273–…	208–250		37.0	39.0	49.5	[a]		49.87	$½N_2 + N_2O$		$½N_2 + N_2O$	$½N_2 + N_2O$		
IIIb	286–320	286–320				13.0	12.0					$+NO + 3H_2O$		$+NO + 3H_2O$	$+NO + 3H_2O$		
	Temperature ranges (°C)					Mass after decomposition (%)						Products of thermal decomposition					
	This study		[20]	[21]	[22]	This study		[20]	[21]	[22]	Calculated	This study		[20]	[21]	[22]	
	Ar	He	Ar	Air	He	Ar	He	Ar	Air	He		Ar	He	Ar	Air	He	
Solid	303–500	320–500	…–477	251–600		27.4	25.8	26.2	[a]	[a]	26.21	NiO		NiO	NiO	NiO	

[a] This value was not presented in the paper

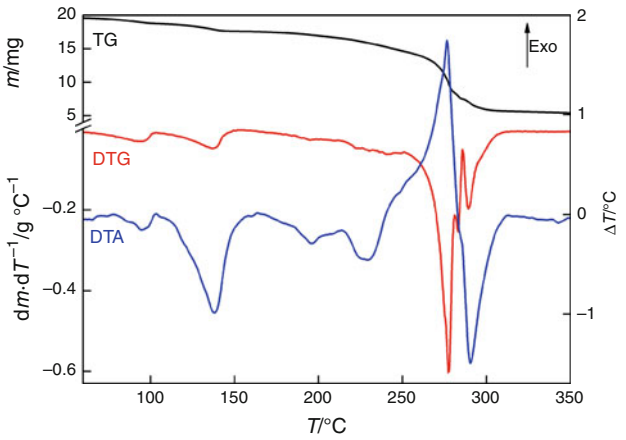

Fig. 6 TG, DTG and DTA curves obtained for thermal decomposition of $[Ni(NH_3)_6](NO_3)_2$ in a flow of He

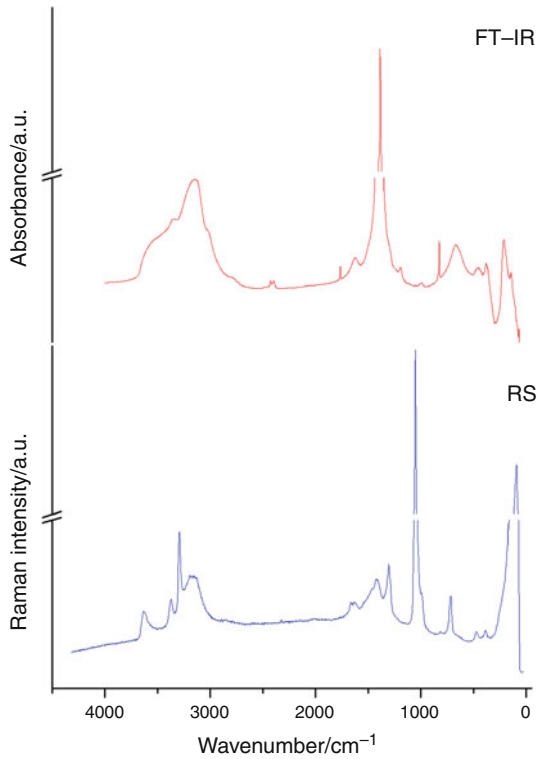

Fig. 7 Comparison of FT-FIR and RS room temperature spectra of $[Ni(NH_3)_6](NO_3)_2$ and $[Ni(NH_3)_2](NO_3)_2$

$[Ni(NH_3)_6](NO_3)_2$, we have repeated thermal decomposition of hexammine complex and stopped this process at 240 °C, similar to what we did in our previous work [20], but this time in He atmosphere. The heated substance changed its colour from bright violet to dark green. After cooling this substance, we performed its chemical and infrared plus Raman spectroscopy analyses, which indicated that both the composition and coordination character of this compound is as such expressed by the

Table 2 The list of band positions of the infrared (IR) and Raman (RS) spectra of $[Ni(NH_3)_6](NO_3)_2$—(**6**) and $[Ni(NH_3)_2](NO_3)_2$—(**2**) at room temperature (*vw* very weak, *w* weak, *sh* shoulder, *m* medium, *s* strong, *vs* very strong, *br* broad, *sp* sharp)

IR			RS			Assignments
6	**2**	NO_3^-	**6**	**2**	NO_3^-	
	3,560 m,br		3,390 m	3,629 s		$\nu_{as}(NH)F_{2g}$
						$\nu_{as}(NH)F_{1u}$
3,346 s	3,355 s,sh					$\nu_{as}(NH)F_{1u}$
			3,295 s	3,368 s		$\nu_s(NH)A_{1g}$
3,242 sh	3,150 s,br					$\nu_s(NH)F_{1u}$
			3,195 w	3,292 vs		$\nu_s(NH)E_g$
	3,016 w,sh					$2\delta_{as}(HNH)F_{1u}$
				3,160 s,br		$2\delta_{as}(HNH)F_{2g}$
1,764 w	1,764 w,sp					$2\nu_2(NO_3^-)A_2''$
				1,662 m		$2\nu_4(NO_3^-)E'$
			1,630 m,br	1,627 m		$\delta_{as}(HNH)F_{2g}$
1,616 m	1,627 m,br					$\delta_{as}(HNH)F_{1u}$
1,383 vs	1,386 vs	1,370	1,350 w,br	1,416 s,br	1,370	$\nu_3(NO_3^-)E'$
			1,350 w,br	1,304 m		$\delta_s(HNH)A_{1g}$
1,192 s	1,193 w,sp		1,204 w,br			$\delta_s(HNH)F_{1u}$
			1,180 w,br			$\delta_s(HNH)E_g$
1,045 vw	1,000 w,br		1,050 vs	1,051 vs	1,049	$\nu_1(NO_3^-)A_1'$
	888 w,sh			991 w		$\nu_2(NO_3^-)A_2''$
826 m	824 s,sp	830		818 vw		$\nu_2(NO_3^-)A_2''$
		719	705 s	721 s	719	$\nu_4(NO_3^-)E'$
677 m	670 s,br					$\rho_r(NH_3)F_{1u}$
374 vw	460 m,br					$\rho_r(NH_3)F_{2u}$
				472 m		$\rho_r(NH_3)F_{2g}$
			370 s	384 m		$\nu_s(NiN)A_{1g}$
327 vw	378 s,sp					$\nu_{as}(NiN)F_{1u}$
			260 sh			$\nu_{as}(NiN)E_g$
			250 s			$\delta_{as}(NNiN)F_{2g}$
223 vw,br	212 s					$\delta_{as}(NNiN)F_{1u}$
			197 sh			$\nu_L(lattice)A_{1g}$
	143 s,sh					$\nu_L(lattice)F_{1u}$
			90 w,sh	92 vs		$\nu_L(lattice)E_g$

formula: $[Ni(NH_3)_2](NO_3)_2$. Figure 7 and Table 2 prove the above statement. Figure 7 presents the infrared (FT-IR) and Raman light scattering (RS) spectra of diamminenickel(II) nitrate(V). Table 2 contains the frequencies in cm^{-1} of the vibrational modes associated with the bands present in these spectra of $[Ni(NH_3)_2](NO_3)_2$, compared with those obtained from the spectra of $[Ni(NH_3)_6](NO_3)_2$.

On subsequent heating of the intermediate product $[Ni(NH_3)_2](NO_3)_2$, we assume that its thermal decomposition may be presented at least as several different reactions, for example:

$$\begin{aligned}\left[Ni(NH_3)_2\right](NO_3)_2 &\leftrightarrow Ni(NO_3)_2 + 2NH_3 \rightarrow NiO + \frac{1}{2}O_2 \\ &+ N_2 + N_2O + 3H_2O \leftrightarrow NiO + \frac{1}{2}N_2 + N_2O + NO \\ &+ 3H_2O, \end{aligned} \quad (4)$$

and some of them are reversible. We suppose that, at the beginning of $[Ni(NH_3)_2](NO_3)_2$ decomposition, the solid nickel nitrate(V) and gaseous ammonia were created, but immediately $Ni(NO_3)_2$ decomposed according to the following several possible reactions:

$$Ni(NO_3)_2 \rightarrow NiO + 2NO_2 + \frac{1}{2}O_2 \leftrightarrow NiO + 2NO + \frac{3}{2}O_2 \leftrightarrow NiO + NO + NO_2 + O_2. \quad (5)$$

Thermal decomposition of $Ni(NO_3)_2$ results in the formation of non-stoichiometric NiO_{1+x}, which can catalyse many redox reactions. Wojciechowski and Małecki [29] indicated that the concentration of Ni^{3+} achieves 1 % of Ni^{2+} concentration. The system of Ni^{3+}/Ni^{2+} with anionic vacancies in the oxide lattice can work as electron and oxygen transmitters between reductive NH_3 molecules and oxidative nitrate ions or nitrogen oxides. The rate of acceleration during final $[Ni(NH_3)_2](NO_3)_2$ decomposition may be caused by an autocatalytic effect of NiO_{1+n} (a mixture of $(1 - n)NiO{\cdot}nNiO_2$, where $n\{0,1\}$).

The products of reactions (4) and (5) can react with each other, for example:

$$2NO + \frac{3}{2}O_2 + 2NH_3 \rightarrow \frac{1}{2}O_2 + N_2 + N_2O + 3H_2O \quad (6)$$

$$NO + NO_2 + O_2 + 2NH_3 \rightarrow +\frac{1}{2}N_2 + N_2O + NO + 3H_2O. \quad (7)$$

It is also a well-known fact that NO, NO_2 and O_2 are in equilibrium with each other, and above 150 °C, the main components are NO and O_2 (and NO_2 is a minor component) and decomposes completely at higher temperatures. It is also sure that in the presence of a catalytically active nickel oxide, NH_3 can reduce the NO_2, O_2 or NO, with the formation of N_2O or N_2, and the N_2O can also react with NH_3.

From the point of view of the probability of the above-presented different reactions which take place during the thermal decomposition of $[Ni(NH_3)_6](NO_3)_2$, and taking into account the QMS analysis results, it is quite reasonable to accept that the final products of this process is as such presented by Eqs. (1–3), and specified in Table 1, where the temperatures, percentage mass losses and the products of the $[Ni(NH_3)_6](NO_3)_2$ thermal decomposition in a flow of Ar and He at the particular stages of this decomposition process are presented . This table also presents the comparison of the results obtained in this study with the results obtained by us earlier [20] for a sample in corundum crucible (in Ar atmosphere) with results of Farhadi and Roostaei-Zaniyani [21] obtained in air atmosphere and with the results of Rejitha et al. [22] obtained in He atmosphere. All measurements were performed at a constant heating rate of 10 °C min^{-1}. Unfortunately, Rejitha et al. did not state what kind of sample container was used and, additionally, and more importantly, these authors did not present the values of the mass loss at particular stages of the decomposition process. As can be seen from this comparison, there are only some small, relatively insignificant differences between our presentation and previous result and between the results obtained by Farhadi and Roostaei-Zaniyani [21]. However, some quite distinct difference can be observed between the above mentioned and Rejitha et al.'s [22] results. These differences concern our IIIa + IIIb and their II and III stages of the decomposition. Namely, in contrary to [22], we propose that the simple release of NH_3 molecules stopped on $[Ni(NH_3)_2](NO_3)_2$, not on $[Ni(NH_3)_4](NO_3)_2$. Moreover, the second difference relies on a composition of the final gaseous products of the decomposition. In our opinion, the composition of $4NH_3 + NO_3^{\bullet} + NO_2$, proposed by Rejitha et al. [22], is barely little probable. First, the authors did not present MS identification of $NO_3^{\bullet}$ radical. Second, this radical can react with NO_2 giving the products which were presented among others by us in Eq. (2).

To summarise, our interpretation of the $[Ni(NH_3)_6](NO_3)_2$ thermal decomposition process is best supported by experimental results rather than the interpretation proposed by Rejitha et al. [22] and, moreover, it is consistent with the results of the structural [2, 10, 12], vibrational [13, 14] and reorientational [1, 9, 11, 16, 18, 19] dynamics investigations of this compound.

Conclusions

The thermal decomposition process of $[Ni(NH_3)_6](NO_3)_2$ undergoes two main stages. First, simple deamination of $[Ni(NH_3)_6](NO_3)_2$ to $[Ni(NH_3)_2](NO_3)_2$ takes place on a step-by-step basis, and $4NH_3$ molecules per formula unit are liberated in two stages (I and II) in four steps (Ia + Ib and IIa + IIb). Then, decomposition of survivor $[Ni(NH_3)_2](NO_3)_2$ undergoes directly to the final decomposition products: NiO_{1+x}, N_2, O_2, nitrogen oxides and H_2O, without the formation of a stable $Ni(NO_3)_2$, because of the autocatalytic effect of the formed NiO_{1+x}. Obtained results were compared both with those published by us earlier and also with the new results published by Rejitha et al. and agreement between our former and present result was obtained. In both cases, $4NH_3$ molecules per formula unit are liberated and the final products of decomposition are the same (N_2, O_2, NO, N_2O, NO_2, H_2O and NiO). However, some disagreement was ascertained when comparing our results with those of Rejitha et al. [22], in which only $2NH_3$ molecules are directly liberated in two steps (stages I and II). Next, in stage III, $[Ni(NH_3)_4](NO_3)_2$ decomposes into $4NH_3 + NO_3^{\bullet} + NO_2 + NiO$. On the other hand, these authors finally concluded that the final products of the $[Ni(NH_3)_6](NO_3)_2$ pyrolysis as N, N_2, O_2, NO, N_2O, H_2O and NiO. So, these products are (but with the exception of N and NO_2) nearly the same as those which we had observed.

Acknowledgements The FT-IR investigations were carried out with the equipment purchased thanks to the financial support of the European Regional Development Fund in the framework of the Polish Innovation Economy Operational Program (Contract No. POIG.02.01.00-12-023/08).

References

1. Janik JM, Janik JA, Migdał-Mikuli A, Mikuli E, Otnes K. Neutron quasielastic scattering results for $[Me(NH_3)_6](XY_4)_2$, $[Me(NH_3)_6](XY_3)_2$ and $[Me(NH_3)_6](XY_2)_2$ compounds, compared with the calorimetric and Raman line width data—a new analysis. Phys B. 1991;168:45–52.
2. Stankowski J. Structural phase transitions in $Me(NH_3)_6X_2$. Mater Sci. 1976;II(3):57–62.
3. Kas'yanenko NA, Afanasieva DA. Conformational changes of DNA molecules in interactions with bioactive compounds. II. DNA complexes with coordination compounds of Cobalt and Ruthenium. J Struct Chem. 2006;47:170–7.
4. Bharanidharan D, Thiyagarajan S, Gautham N. Hexammineruthenium(III) ion interactions with Z-DNA. Acta Crystallogr. 2007;F63:1008–13.
5. Reedijk J. New clue for platinum antitumor chemistry: kinetically controlled metal binding to DNA. Proc Natl Acad Sci USA. 2003;100:3611–6.
6. Sørensen RZ, Hummelshøj JS, Klerke A, Revers JB, Vegge T, Norskøv JK, Christensen CH. Indirect, reversible high-density hydrogen storage in compact ammine salts. J Am Chem Soc. 2008;130:8660–8.
7. Elmøe TD, Sørensen RZ, Quaade UJ, Christensen CH, Nørskov JK, Johannessen T. A high-density ammonia storage/delivery system based on $Mg(NH_3)_6Cl_2$ for SCR–DeNO(x) in vehicles. Chem Eng Sci. 2006;61:2618–25.
8. Migdał-Mikuli A, Mikuli E, Rachwalska M, Stanek T, Janik JM, Janik JA. An adiabatic calorimetry study of $[Ni(NH_3)_6](NO_3)_2$. Phys B. 1981;104:331–6.
9. Janik JA, Janik JM, Migdał-Mikuli A, Mikuli E, Stanek T. Comparison of calorimetry and neutron scattering results concerning phase transitions in $[Ni(NH_3)_6](NO_3)_2$ with the Raman band profile study. J Mol Struct. 1984;115:5–10.
10. Andresen AF, Fjelvåg H, Janik JA, Mayer J, Ściesiński J, Janik JM, Migdał-Mikuli A, Mikuli E, Rachwalska M, Stanek T. Adiabatic calorimetry and neutron diffraction studies of phases and phase transitions in $[Ni(ND_3)_6](NO_3)_2$. Phys B. 1986;138:295–304.
11. Migdał-Mikuli A, Mikuli E. Connection between reorientational motions of NH_3 groups and phase transitions in $[Ni(NH_3)_6](NO_3)_2$ and $[Mg(NH_3)_6](NO_3)_2$ compounds. Acta Phys Polon A. 1995;88:527–32.
12. Hodorowicz S, Czerwonka J, Janik JM, Janik JA. X-ray powder diffraction studies of the thermal transformations in solid $[Ni(NH_3)_6](NO_3)_2$. Phys B. 1981;111:155–9.
13. Isotani S, Sano W, Ochi JA. Phase transition in metal hexammine complexes. I. The infrared spectra of $Ni(NH_3)_6(NO_3)_2$. J Phys Chem Solids. 1975;36:95–8.
14. Jenkins TE, Ferris LTH, Bates AR, Gillard RD. A Raman study of the orientational phase transitions of hexammine nickel(II) nitrate. J Phys C. 1978;11:L77–9.
15. Piekara-Sady L, Krupski M, Stankowski J, Gajda D. Evidence of hydrogen bonds in $[Ni(NH_3)_6](NO_3)_2$. Phys B. 1986;138:118–24.
16. Fimland BO, How T, Svare I. Nitrate motions and dielectric losses in nickel hexammine nitrate. Phys Scripta. 1986;33:456–8.
17. Stankowski J, Trybuła Z. Phase transitions in $[Ni(NH_3)_6](NO_3)_2$. Phys B. 1988;154:87–92.
18. Czaplicki J, Weiden N, Weis A. NMR proton relaxation in $Ni(NH_3)_6(NO_3)_2$. Phys B. 1988;154:93–6.
19. Kearley GJ, Blank H. NH_3 reorientations in phases I, II and III of $Ni(NH_3)_6(NO_3)_2$. Can J Chem. 1988;66:692–7.
20. Migdał-Mikuli A, Mikuli E, Dziembaj R, Majda D, Hetmańczyk Ł. Thermal decomposition of $[Mg(NH_3)_6](NO_3)_2$, $[Ni(NH_3)_6](NO_3)_2$ and $[Ni(ND_3)_6](NO_3)_2$. Thermochim Acta. 2004;419:223–9.
21. Farhadi S, Roostaei-Zaniyani Z. Simple and low temperature synthesis of NiO nanoparticles through solid-state thermal decomposition of the hexa(ammine)Ni(II) nitrate, $[Ni(NH_3)_6](NO_3)_2$, complex. Polyhedron. 2011;30:1244–9.
22. Rejitha KS, Ichikawa T, Mathew S. Investigation of the thermal behaviour of $[Ni(NH_3)_6](NO_3)_2$ and $[Ni(en)_3](NO_3)_2$ using TG-MS and TR-XRD under inert condition. J Therm Anal Calorim. 2012;107:887–92.
23. Mikuli E, Migdał-Mikuli A, Chyży, Grad B, Dziembaj R. Melting and thermal decomposition of $[Ni(H_2O)_6](NO_3)_2$. Thermochim Acta. 2001;370:65–71.
24. Mikuli E, Liszka M, Molenda M. Thermal decomposition of $[Cd(NH_3)_6](NO_3)_2$. J Therm Anal Calorim. 2007;89:573.
25. Liszka-Skoczylas M, Mikuli E, Szklarzewicz J, Hetmańczyk J. Thermal behaviour, phase transitions and molecular motions in $[Co(NH_3)_6](NO_3)_2$. Thermochim Acta. 2009;496:38–44.
26. Mikuli E, Liszka-Skoczylas M, Hetmańczyk J, Szklarzewicz J. Thermal properties, phase transitions, vibrational and reorientational dynamics of $[Mn(NH_3)_6](NO_3)_2$. J Therm Anal Calorim. 2010;102:889–97.
27. L'vov BV, Novichikhin AV. Mechanism of thermal decomposition of anhydrous metal nitrates. Spectrochim Acta B. 1995;50:1425–48.
28. Ettarh C, Galwey A. A kinetic and the mechanistic study of the thermal decomposition of calcium nitrate. Thermochim Acta. 1996;288:203–19.
29. Wojciechowski KT, Małecki A. Mechanism of thermal decomposition of cadmium nitrate $Cd(NO_3)_2{\cdot}4H_2O$. Thermochim Acta. 1999;331:73–7.
30. Małecki A, Gajerski R, Łabuś S, Prochowska-Klich B, Wojciechowski KT. Mechanism of thermal decomposition of *d*-metals nitrates hydrates. J Thermal Anal Calorim. 2000;60:17–23.
31. Małecki A, Małecka B. Formation of N_2O during thermal decomposition of *d*-metal hydrates nitrates. Thermochim Acta. 2006;446:113–6.
32. Rodrigues ACC, Monteiro JLF. Thermal decomposition of $[Pt(NH_3)_4]^{2+}$ complex in NaX zeolite: effect of calcinations procedure. J Therm Anal Calorim. 2006;83:451–5.
33. Mádarász J, Bombicz P, Mátyás C, Réti F, Kiss G, Pokol G. Comparative evolved gas analytical and structural study on *trans*-diammine-bis(nitrito)-palladium(II) and platinum(II) by TG/DTA-MS, TG-FTIR, and single crystal X-ray diffraction. Thermochim Acta. 2009;490:51–9.
34. Sajó IE, Kótai L, Keresztury G, Gács I, Pokol G, Kristóf J, Soptrayanov B, Petrusevski VM, Timpu D, Sharma PK. Studies on the chemistry of tetraamminezinc(II) dipermanganate ($[Zn(NH_3)_4]$ $(MnO_4)_2$): low-temperature synthesis of the manganese zinc oxide ($ZnMn_2O_4$) catalyst precursor. Helv Chim Acta. 2008;91:1646–58.

35. Kótai L, Banerji KK, Sajó I, Kristóf J, Sreedhar B, Holly S, Keresztury G, Rockenbauer A. An unprecedented-type intramolecular redox reaction of solid tetraamminecopper(2+) bis(permanganate) ($[Cu(NH_3)_4](MnO_4)_2$)—a low-temperature synthesis of copper dimanganese tetraoxide-type ($CuMn_2O_4$) nanocrystalline catalyst precursors. Helv Chim Acta. 2002;85:2316–27.

36. Kótai L, Sajó IE, Jakab E, Keresztury G, Németh C, Gács I, Menyhárd A, Kristóf J, Hajba L, Petrusevski VM, Ivanovski V, Timpu D, Sharma PK. Studies on the chemistry of $[Cd(NH_3)_4](MnO_4)_2$. A low temperature synthesis route of the $CdMn_2O_{4+x}$ type NO_x and CH_3SH sensor precursors. Z Anorg Allg Chem. 2012;638:177–86.